Research Square

Preprints are preliminary reports that have not undergone peer review.
They should not be considered conclusive, used to inform clinical practice,
or referenced by the media as validated information.

Three-Dimensional CBCT Assessment of Buccal and Lingual/Palatal Bone Thickness Surrounding Developing Permanent Tooth Germs in Pediatric Patients

Hasan Said Şener
Dicle University
Mehmet Emin Dogan
Harran University
Şeyda Alkan
Harran University
Yelda Polat Yavuz
Dicle University
Demet Süer Tümen
Dicle University
İlhan Şengül
Harran University
Menduh Sercan Kaya
Dicle University
Emin Caner Tümen
ect1976@gmail.com

Dicle University

Research Article

Keywords: cone-beam computed tomography, permanent tooth germ, bone thickness, alveolar bone development

Posted Date: October 27th, 2026

DOI: https://doi.org/10.21203/rs.3.rs-11254591/v1

License: This work is licensed under a Creative Commons Attribution 4.0 International License.
Read Full License

Additional Declarations: No competing interests reported.

Abstract

Background

The anatomical relationship between developing permanent tooth germs and the surrounding cortical bone changes during growth and may be relevant to pediatric surgical and orthodontic procedures. This study aimed to evaluate buccal and lingual/palatal bone thickness surrounding developing permanent tooth germs using cone-beam computed tomography (CBCT) and to assess the effects of age, sex, and tooth type.

Methods

This retrospective cross-sectional study included CBCT images of 106 children aged 6–12 years. Bilateral permanent canines, first and second premolars, and second molars were evaluated. Buccal bone thickness (BBT) and lingual/palatal bone thickness (L/PBT) were measured on axial sections. Statistical analyses included the Kolmogorov–Smirnov test, Mann–Whitney U test, paired-samples t-test, and Spearman correlation analysis ($p < 0.05$).

Results

The mean age was 9.19 ± 1.61 years. Sex-related differences were limited, and contralateral symmetry was generally maintained ($p > 0.05$). Significant age-related changes were observed in several regions. In the maxilla, palatal bone thickness decreased with age, with the strongest negative correlation observed for tooth 24 (rho = − 0.505, $p < 0.001$). In the mandible, age was negatively correlated with buccal bone thickness of teeth 33, 34, and 45, whereas positive correlations were observed for buccal bone thickness of tooth 37 and lingual bone thickness of teeth 43, 44, and 47.

Conclusions

Bone thickness surrounding developing permanent tooth germs varies according to tooth type, jaw region, and age. These age-related differences reflect dentoalveolar remodeling during growth, while sex has a limited influence and contralateral symmetry is generally preserved. These findings provide anatomical reference data that may support risk assessment and treatment planning during the mixed dentition period.

1. Introduction

The basis of clinical success in dental treatments depends on a correct diagnosis and the careful planning of the treatment that follows. The integration of Cone-Beam Computed Tomography (CBCT) into dental practices has enabled clinicians to access three-dimensional, high-resolution images of

dentofacial structures through a non-invasive approach. Unlike conventional two-dimensional radiographs, CBCT eliminates the superimposition of anatomical structures, allowing for a detailed evaluation of the labial/buccal and lingual alveolar bone surfaces [1]. This is of paramount importance in the treatment of pediatric patients in the mixed dentition period. Accurate assessment of the intraosseous position of erupting permanent teeth provides valuable information for patient-specific treatment planning and clinical decision-making [2].The tooth germs of erupting young permanent teeth are located in close proximity to the cortical bones during the early stages of their development. As development progresses, the dental follicle expands symmetrically in buccal, occlusal, and apical directions; active eruption begins once crown formation is complete and the root length reaches approximately 2–4 mm. During this process, bone resorption occurs in the bone along the eruption pathway of the tooth, while bone apposition takes place in the region of the root, thereby continuously altering the position of the tooth within the jaw. This dynamic process of development and remodeling renders the clinical evaluation of the positions of developing permanent tooth germs within the alveolar bone, as well as their relationships with the surrounding bone structures, highly significant [3, 4].

Most of the studies available in the literature have focused on erupted teeth or third molar tooth germs because of their association with common clinical problems. Studies on other permanent tooth germs in pediatric patients are limited [5, 6]. In particular, few studies have evaluated their positional relationships, distances to surrounding structures, and adjacent bone thickness. Because most current studies are based on adult data, a significant information gap remains in establishing reference anatomical values for children during active growth and development [7]. Evaluating anatomical relationships between developing permanent tooth germs and surrounding bone is essential for understanding growth processes and guiding clinical practice. These insights help identify anatomical risks during the pre-eruptive period, supporting the planning of surgical interventions and early orthodontic treatments. Furthermore, CBCT imaging accurately reveals bone structures surrounding tooth germs in three dimensions, providing detail on potential perforation risks and relationships with neighboring structures [8].

Consequently, this descriptive and associational study establishes a 3D anatomical reference set for developing canines, premolars, and second molars using CBCT. We quantitatively evaluated buccal and lingual/palatal bone thicknesses and examined the effects of age, sex, and jaw region on these dimensions. We hypothesized that cortical bone thickness varies significantly by tooth type and jaw region and changes with age, while the influence of sex remains limited. By extending evaluations beyond third molars, this study provides an incremental but meaningful contribution to defining developmental boundaries in a mixed-dentition population. These findings provide an anatomical baseline to support risk assessment and treatment planning in pediatric dentistry, orthodontics and oral surgery.

2. Materials and Methods

2.1. Study Design and Ethical Approval

Archived CBCT records of pediatric individuals were analyzed in this retrospective cross-sectional study. These records were previously obtained for diagnostic and treatment purposes. The study protocol was approved by the local Clinical Research Ethics Committee, and the research adhered to the ethical principles of the Declaration of Helsinki.

2.2. Sample Selection

CBCT images obtained between 2022 and 2024 for diagnostic evaluation and treatment planning purposes were retrospectively reviewed. Previously acquired CBCT scans of pediatric patients aged 6–12 years, in whom developing permanent tooth germs could be observed, were evaluated for inclusion in the study.

The inclusion criteria were defined as follows: being between the ages of 6 and 12 years at the time of the CBCT scan; the presence of developing permanent canine, first premolar, second premolar, and second molar tooth germs in the maxilla and/or mandible; the availability of high-quality CBCT records allowing adequate evaluation of the cortical bone borders and tooth germs; and the absence of image artifacts that could affect the diagnostic evaluation.

The exclusion criteria were defined as a history of trauma or surgical intervention in the maxillofacial region; the presence of previous or ongoing orthodontic treatment; craniofacial syndromes, cleft lip and/or palate, or systemic diseases that could affect craniofacial growth and bone metabolism; the presence of bone pathologies that could alter normal anatomical structures; the presence of motion artifacts, metal artifacts, or incomplete CBCT datasets; the presence of tooth germs associated with odontomas, supernumerary teeth, or other developmental anomalies; and instances where the tooth evaluated on CBCT images was completely erupted or the tooth germ had completed its development to an extent that precluded evaluation.

2.3. Sample Size and Power Analysis

The minimum sample size was calculated using G*Power software (Version 3.1.9.7; Heinrich Heine University, Düsseldorf, Germany). Initially, a power analysis for correlation analysis indicated that 64 cases were required, based on an effect size of 0.30, a significance level (α) of 0.05, and 80% power. A second power analysis for intergroup comparisons (independent samples t-test or Mann–Whitney U test) required at least 106 cases, assuming an effect size of 0.50, a significance level (α) of 0.05, and 80% power. Because both analyses were performed in this study, the calculation requiring the larger sample size was used as the basis, and the minimum sample size was determined to be 106 cases. Although 106 CBCT scans were initially included, the final analytical population for each tooth-specific measurement varied. After case inclusion, individual tooth germs were excluded site-specifically if the tooth was erupted, congenitally absent, or if localized motion artifacts and poor image clarity precluded precise anatomical evaluation. Only fully evaluable observations were included in the respective site-specific analyses, resulting in the varying sample sizes (n) reported in Tables 2 and 4.

2.4. CBCT Imaging Protocol

All CBCT images were acquired using a Castellini X-Radius Trio Plus (Imola, Italy) device. The imaging parameters were set at 90 kVp and 16 mAs. The images were recorded with a voxel size of 0.3 mm and a field of view (FOV) of 13 × 16 cm and 13 × 10 cm. The DICOM data were reconstructed at a slice thickness of 0.3 mm using IRYS Viewer 15.1 software.

2.5. Standardization of Images and Measurement Procedure

CBCT images were evaluated in axial, coronal, and sagittal planes using IRYS Viewer 15.1 software. This study examined developing permanent tooth germs (13, 14, 15, 17, 23, 24, 25, 27, 33, 34, 35, 37, 43, 44, 45, and 47) bilaterally in the maxilla and mandible. Each tooth germ was first evaluated in the coronal slice to identify the level of its widest buccolingual diameter, which was defined as the equator line. Subsequent measurements were performed on the corresponding axial slice.

Bone thickness adjacent to the tooth germs was evaluated using the shortest-distance approach described in previous CBCT studies of teeth, tooth germs, and other odontogenic structures. Accordingly, bone thickness was defined as the shortest linear distance (measured in millimeters) between the outer surface of the tooth germ crown and the outer boundary of the adjacent cortical bone (Fig. 1). Buccal and palatal thicknesses were recorded separately for maxillary teeth, while buccal and lingual thicknesses were recorded for mandibular teeth. For multi-rooted teeth, measurements were based on the shortest linear distance from the outer contour of the tooth germ crown to the respective cortical bone boundary. All measurements were performed under standardized conditions using the same software.

In Fig. 1, the red, green, and blue lines indicate the coronal, sagittal, and axial planes, respectively. Turquoise lines represent the buccal and lingual/palatal bone thicknesses, measured at the equator level determined in the coronal slice. The measurements were performed so that the measurement line was as perpendicular to the bone surface as possible to ensure geometric accuracy.

2.6. Reliability Analysis

To ensure measurement reproducibility, 25 randomly selected CBCT scans (approximately 23% of the total sample) were re-evaluated by the same examiner after a four-week interval. The primary objective was to confirm the consistency of the shortest-distance measurements used throughout the study.

2.7. Statistical Analysis

Statistical analysis of the study data was performed using IBM SPSS Statistics for Windows, Version 25.0 (IBM Corp., Armonk, NY, USA) software. For descriptive statistics, mean, standard deviation, number, and percentage values were calculated. The conformity of the data to normal distribution was evaluated using the Kolmogorov–Smirnov test. For bilateral (right-versus-left) comparisons, the normality of the distribution of paired differences was assessed using the Shapiro-Wilk test. Since the paired differences for the majority of measurements exhibited a normal distribution, the paired-samples

t-test was employed to evaluate bilateral symmetry. For any measurement where the assumption of normality for paired differences was not met, the non-parametric Wilcoxon signed-rank test was used to ensure inferential appropriateness.

For comparisons between sexes, the Mann–Whitney U test was applied as the data did not show a normal distribution. The statistical analyses in this study were considered exploratory given the descriptive nature of the research and the multiple parallel hypothesis tests conducted; therefore, no formal multiplicity adjustments (e.g., Bonferroni correction) were applied. Spearman correlation analysis was used to evaluate the relationship between age and measurements. In this context, all age-related analyses represent cross-sectional associations observed between different children of various ages rather than longitudinal evidence of individual developmental trajectories over time. The magnitude of the observed correlations and mean differences was interpreted according to standard effect-size conventions (rho 0.1–0.3 small, 0.3–0.5 moderate, > 0.5 strong). Furthermore, reporting completeness was ensured by including 95% confidence intervals (CIs) for principal inferential analyses. Intra-observer reliability was assessed using an Intraclass Correlation Coefficient (ICC) based on a two-way mixed-effects model with absolute agreement, which yielded a value of 0.808, indicating good reliability. The statistical significance level was accepted as $p < 0.05$.

3. Results

The site-specific analyses were performed using the subset of evaluable observations available for each measurement; therefore, the sample sizes reported in the tables vary by tooth type and jaw region according to the eligibility criteria defined in the Methods.

3.1. Participant Characteristics

A total of 106 CBCT scans from pediatric individuals were included in the study. The mean age of the participants was 9.19 ± 1.61 years, ranging from 6 to 12 years. Buccal bone thickness (BBT) and lingual/palatal bone thickness (L/PBT) measurements were performed in regions adjacent to the permanent tooth germs in all individuals.

3.2. Descriptive Statistics

Descriptive statistics of the buccal and lingual/palatal bone thickness measurements associated with the tooth germs are presented in Table 1. Bone thickness values showed considerable variation according to tooth type and jaw region. In the maxilla, the lowest buccal bone thickness was observed in the canine tooth germ regions (13B: 0.67 ± 0.41 mm; 23B: 0.68 ± 0.69 mm), whereas the greatest palatal bone thickness was also recorded in the canine regions (13P: 3.94 ± 2.58 mm; 23P: 3.72 ± 2.48 mm). In the maxillary premolar regions, buccal and palatal bone thicknesses exhibited a more balanced distribution; however, an increase in buccal bone thickness was noted around the second premolar tooth germs (15B: 2.01 ± 1.38 mm; 25B: 2.03 ± 1.52 mm).

In the mandible, buccal bone thickness values were generally below 1 mm in the anterior and first premolar regions, whereas higher values were observed in the second premolar and second molar regions (35B: 1.46 ± 0.81 mm; 37B: 1.79 ± 0.82 mm; 45B: 1.40 ± 0.80 mm; 47B: 1.71 ± 0.74 mm). Regarding lingual bone thickness, the lowest values were detected in the mandibular second molar regions (37L: 0.96 ± 0.45 mm; 47L: 1.03 ± 0.50 mm) (Table 1).

Table 1
Descriptive Statistics of Buccal and Lingual/Palatal Bone Thickness Measurements Adjacent to Permanent Tooth Germs (mm)

Permanent Tooth Germ	Buccal Bone Thickness (mm) (Mean ± SD)	Lingual/Palatal Bone Thickness (mm) (Mean ± SD)
13	0.67 ± 0.41	3.94 ± 2.58
14	0.74 ± 0.67	1.90 ± 1.43
15	2.01 ± 1.38	1.99 ± 1.12
17	1.01 ± 0.56	2.51 ± 1.35
23	0.68 ± 0.69	3.72 ± 2.48
24	0.63 ± 0.49	1.46 ± 1.04
25	2.03 ± 1.52	1.87 ± 0.97
27	0.94 ± 0.57	2.31 ± 1.25
33	0.66 ± 0.41	1.78 ± 1.03
34	0.71 ± 0.45	1.49 ± 0.91
35	1.46 ± 0.81	1.24 ± 0.67
37	1.79 ± 0.82	0.96 ± 0.45
43	0.77 ± 0.38	1.83 ± 0.90
44	0.80 ± 0.40	1.67 ± 0.73
45	1.40 ± 0.80	1.21 ± 0.59
47	1.71 ± 0.74	1.03 ± 0.50

Descriptive statistics are presented as mean ± standard deviation. PBT was reported for maxillary teeth, whereas LBT was reported for mandibular teeth. BBT: buccal bone thickness; PBT: palatal bone thickness; LBT: lingual bone thickness; Mean: mean; SD: standard deviation.

3.3. Sex-Based Comparisons

Sex-based comparisons revealed no significant differences between males and females for the majority of measurement sites ($p > 0.05$). A statistically significant difference was observed only for the buccal

bone thickness of the mandibular left second premolar tooth germ (35B), which was greater in males than in females (1.71 ± 0.84 mm vs. 1.22 ± 0.72 mm, respectively; p = 0.005). No significant sex-related differences were detected in any of the remaining measurements (Table 2).

Table 2
Comparison of Buccal and Lingual/Palatal Bone Thickness Measurements According to Sex

Measurement Parameter	Male (n)	Male Mean ± SD (mm)	Female (n)	Female Mean ± SD (mm)	p-value
13-BBT	47	0.67 ± 0.37	32	0.67 ± 0.48	0.962
13-PBT	47	4.01 ± 2.61	32	3.83 ± 2.56	0.769
14-BBT	32	0.81 ± 0.80	23	0.64 ± 0.41	0.360
14-PBT	33	2.18 ± 1.61	23	1.50 ± 1.02	0.084
15-BBT	44	1.96 ± 1.21	33	2.08 ± 1.61	0.720
15-PBT	44	2.09 ± 1.14	33	1.86 ± 1.10	0.376
17-BBT	53	1.06 ± 0.51	38	0.94 ± 0.62	0.289
17-PBT	53	2.55 ± 1.43	38	2.46 ± 1.26	0.731
23-BBT	48	0.72 ± 0.57	35	0.63 ± 0.82	0.570
23-PBT	49	3.88 ± 2.35	35	3.50 ± 2.67	0.489
24-BBT	36	0.69 ± 0.48	27	0.54 ± 0.48	0.228
24-PBT	36	1.59 ± 0.95	27	1.28 ± 1.15	0.254
25-BBT	45	2.05 ± 1.60	34	2.00 ± 1.42	0.877
25-PBT	45	1.83 ± 0.85	34	1.91 ± 1.12	0.706
27-BBT	53	0.98 ± 0.49	37	0.88 ± 0.68	0.421
27-PBT	53	2.41 ± 1.20	37	2.17 ± 1.32	0.370
33-BBT	44	0.68 ± 0.38	33	0.63 ± 0.46	0.600
33-LBT	44	1.71 ± 0.95	33	1.87 ± 1.14	0.516
34-BBT	38	0.74 ± 0.49	34	0.68 ± 0.40	0.540
34-LBT	38	1.52 ± 0.91	34	1.45 ± 0.92	0.744
35-BBT	42	1.71 ± 0.84	43	1.22 ± 0.72	0.005
35-LBT	42	1.25 ± 0.65	40	1.23 ± 0.71	0.919
37-BBT	47	1.89 ± 0.89	38	1.68 ± 0.73	0.249
37-LBT	47	1.00 ± 0.42	38	0.91 ± 0.48	0.404
43-BBT	42	0.80 ± 0.40	28	0.72 ± 0.35	0.433
43-LBT	42	1.80 ± 0.87	28	1.89 ± 0.95	0.670

Measurement Parameter	Male (n)	Male Mean ± SD (mm)	Female (n)	Female Mean ± SD (mm)	p-value
44-BBT	32	0.78 ± 0.39	30	0.83 ± 0.42	0.684
44-LBT	32	1.67 ± 0.84	30	1.66 ± 0.62	0.964
45-BBT	42	1.45 ± 0.90	39	1.34 ± 0.68	0.534
45-LBT	42	1.30 ± 0.61	39	1.12 ± 0.55	0.176
47-BBT	46	1.77 ± 0.84	39	1.64 ± 0.62	0.413
47-LBT	46	1.09 ± 0.53	39	0.95 ± 0.46	0.186

The Mann–Whitney U test was used for statistical comparisons. BBT: buccal bone thickness; PBT: palatal bone thickness; LBT: lingual bone thickness; Mean: mean; SD: standard deviation. n: Represents the number of evaluable tooth germs available for analysis at each anatomical site. Variations in sample size (n) across teeth and regions are attributable to site-specific exclusions, including tooth eruption, congenital absence (agenesis), and inadequate image quality, as described in the Materials and Methods section.

3.4. Bilateral Comparisons

Bilateral symmetry was highly preserved across the evaluated regions, with no statistically significant differences observed between the right and left sides for any of the buccal or lingual/palatal bone thickness measurements associated with corresponding tooth germs ($p > 0.05$; Table 3).

Table 3
Comparison of Buccal and Lingual/Palatal Bone Thickness Measurements Between the Right and Left Sides

Tooth Site	Parameter	Right Mean ± SD (mm)	Left Mean ± SD (mm)	p-value
13–23	BBT	0.66 ± 0.41	0.71 ± 0.68	0.582
13–23	PBT	3.97 ± 2.58	3.99 ± 2.36	0.914
14–24	BBT	0.75 ± 0.69	0.74 ± 0.46	0.907
14–24	PBT	1.78 ± 0.99	1.60 ± 0.88	0.167
15–25	BBT	2.04 ± 1.40	2.04 ± 1.49	0.984
15–25	PBT	2.02 ± 1.14	1.86 ± 0.85	0.200
17–27	BBT	1.01 ± 0.56	0.94 ± 0.57	0.230
17–27	PBT	2.49 ± 1.34	2.31 ± 1.25	0.142
33–43	BBT	0.73 ± 0.37	0.76 ± 0.38	0.504
33–43	LBT	1.96 ± 0.91	1.83 ± 0.90	0.155
34–44	BBT	0.80 ± 0.40	0.81 ± 0.41	0.848
34–44	LBT	1.70 ± 0.80	1.67 ± 0.72	0.601
35–45	BBT	1.52 ± 0.79	1.41 ± 0.80	0.143
35–45	LBT	1.25 ± 0.67	1.22 ± 0.59	0.554
37–47	BBT	1.80 ± 0.83	1.70 ± 0.75	0.148
37–47	LBT	0.96 ± 0.45	1.02 ± 0.50	0.233

Statistical comparisons were performed using the paired-samples t-test. BBT: buccal bone thickness; PBT: palatal bone thickness; LBT: lingual bone thickness; Mean: mean; SD: standard deviation.

3.5. Correlation Analysis with Age

The relationship between age and bone thickness measurements was evaluated using Spearman's correlation analysis. In the maxillary region, significant negative correlations were found between age and palatal bone thickness measurements of teeth 14, 15, 17, 24, and 27 (rho ranging from − 0.225 to − 0.505; $p < 0.05$). Buccal bone thickness measurements of teeth 23 and 24 were also negatively correlated with age. The strongest correlation was found for palatal bone thickness of tooth 24 (rho = − 0.505; $p < 0.001$). In the mandibular region, significant negative correlations were found between age and buccal bone thickness measurements of teeth 33, 34, and 45. In contrast, significant positive correlations were observed between age and the buccal bone thickness of tooth 37 as well as the lingual bone thickness measurements of teeth 43, 44, and 47 ($p < 0.05$). The correlation coefficients and corresponding p-values are presented in Table 4.

Table 4
Spearman Correlation Analysis Between Age and Buccal and Lingual/Palatal Bone Thickness Measurements

Measurement Paramater	n	Spearman rho	p value
13-BBT	79	-0.130	0.254
13-PBT	79	0.090	0.431
14-BBT	55	0.000	0.999
14-PBT	56	-0.293	0.028
15-BBT	77	-0.044	0.703
15-PBT	77	-0.328	0.004
17-BBT	91	0.147	0.166
17-PBT	91	-0.294	0.005
23-BBT	83	-0.255	0.020
23-PBT	84	-0.143	0.195
24-BBT	63	-0.302	0.016
24-PBT	63	-0.505	< 0.001
25-BBT	79	0.031	0.789
25-PBT	79	-0.217	0.055
27-BBT	90	0.131	0.218
27-PBT	90	-0.225	0.033
33-BBT	77	-0.437	< 0.001
33-LBT	77	0.084	0.467
34-BBT	72	-0.381	0.001
34-LBT	72	0.034	0.779
35-BBT	85	-0.195	0.073
35-LBT	82	0.020	0.858
37-BBT	85	0.229	0.035
37-LBT	85	0.096	0.382
43-BBT	70	-0.180	0.137
43-LBT	70	0.399	0.001

Measurement Paramater	n	Spearman rho	p value
44-BBT	62	-0.183	0.156
44-LBT	62	0.284	0.025
45-BBT	81	-0.243	0.029
45-LBT	81	0.084	0.455
47-BBT	85	0.175	0.109
47-LBT	85	0.284	0.008

Spearman correlation analysis was performed. Statistically significant values are shown in bold. BBT: buccal bone thickness; PBT: palatal bone thickness; LBT: lingual bone thickness. n: Represents the number of evaluable tooth germs available for analysis at each anatomical site. Variations in sample size (n) across teeth and regions are attributable to site-specific exclusions, including tooth eruption, congenital absence (agenesis), and inadequate image quality, as described in the Materials and Methods section.

4. Discussion

Evaluating the buccal and lingual/palatinal bone thicknesses surrounding tooth germs at a millimeter level using CBCT provides critical clinical insights for determining safe margins in surgical interventions, directing biomechanical forces accurately, and preventing developmental complications [7, 11]. Such quantitative analyses may contribute to anatomical risk assessment and treatment planning in pediatric surgical and orthodontic practice [12, 13]. In our study, the replication of all measurements by a single observer at two different time points and the high level of intra-observer agreement support the reproducibility and methodological reliability of the measurements. Similarly, it is reported in the literature that high ICC values represent a significant methodological strength that increases the reliability of CBCT-based measurements [11].

This study provides an incremental but meaningful contribution to the pediatric maxillofacial anatomy literature by establishing a set of pediatric pre-eruptive reference measurements for developing canines, premolars, and second molars using CBCT. While the existing literature has predominantly focused on erupted teeth in adult individuals [14, 15] or exclusively on mandibular third molar tooth germs [5], our findings help define developmental boundary conditions in a mixed-dentition population. By extending the scope of evaluation beyond third molars to include canines and premolars, this research offers a detailed anatomical framework for the pre-eruptive period, which is essential for understanding ongoing dentoalveolar remodeling during growth.

The findings obtained indicate that the tooth germs are positioned in close proximity to the cortical bone borders. This finding is consistent with previous CBCT observations demonstrating dynamic anatomical relationships between unerupted teeth, their surrounding follicular structures, and the gubernacular tract

during dental development [3, 4]. This anatomical proximity is a condition that warrants clinical consideration, particularly in the pediatric age group, regarding cortical bone perforation, the spread of infection, and surgical complications.

From a clinical perspective, one of the most relevant findings of the present study was the palatal bone thickness of 3.94 ± 2.58 mm observed adjacent to the maxillary canine germs. Previous CBCT studies have demonstrated marked site-specific differences between buccal and palatal alveolar bone dimensions, highlighting the importance of considering the surrounding bony envelope during orthodontic treatment planning [16–18]. On the other hand, the lingual bone thickness in the mandibular second molar region was as low as 0.96 ± 0.45 mm, identifying this region as a potential anatomical risk indicator that may warrant careful assessment to minimize the possibility of lingual cortical perforation during surgical interventions.

Porto et al. reported a lingual bone thickness of 2.95 ± 1.16 mm in the mandibular second molar region of adults, whereas the submillimeter values observed in the present pediatric population demonstrate that lingual bone support during the developmental period is substantially more limited than in adults [18]. These findings underscore the importance of careful anatomical risk assessment when planning surgical and orthodontic procedures in pediatric patients.

Measurements for the right and left homologous tooth germ were similar, reinforcing the methodological strength of our study. This observation is consistent with symmetry results reported in similar CBCT studies on adult populations, suggesting that the development of alveolar bone in healthy individuals is symmetrical and physiological along the dental arch [14, 18, 19]. This symmetry confirms the reliability of our measurement protocol.

When evaluated according to sex, a significant difference was identified in only one of the 32 measurement sites examined. Specifically, the buccal bone thickness of the mandibular left second premolar region (35B) was significantly greater in males than in females (1.71 ± 0.84 mm vs. 1.22 ± 0.72 mm, respectively; $p = 0.005$). Previous studies in adult populations have reported sex-related differences in alveolar bone thickness at specific anatomical sites. Adıgüzel et al. [15] and Firincioglulari et al. [20] reported greater bone thickness in males at several evaluated sites, while the meta-analysis by Shafizadeh et al. [16] identified significant sex-related associations at selected measurement points rather than a uniform pattern across the dentition.

In contrast, bone thicknesses showed no significant sex-related differences at most sites, with the exception of 35B. This finding supports the hypothesis that sex-related differences become more pronounced after puberty due to hormonal changes, skeletal maturation, and increased occlusal forces. This finding may partly reflect developmental differences that become more pronounced during and after puberty, when sex-related differences in bone morphology emerge [22]. Maximum bite force has also been associated with alveolar bone thickness and morphology [21]. Contralateral symmetry during childhood further suggests that growth patterns have not yet undergone sex-specific differentiation at this stage.

Age-related correlation analyses in our study revealed that alveolar bone thickness does not exhibit a static structure throughout the growth process but rather undergoes dynamic changes with age. It should be emphasized that these findings represent cross-sectional associations across children of different ages, not longitudinal evidence of individual remodeling trajectories. The negative correlation observed with age in the palatal bone thickness of maxillary premolars and molars may be associated with the arch expansion accompanying maxillary growth and the buccal and occlusal movements of tooth germs during the eruption process. It is thought that the dentoalveolar remodeling occurring during this period contributes to the observed decrease in palatal bone thickness over time.

A different trend was observed in the mandible; a positive correlation with age was detected in the buccal region of tooth number 37 and in the lingual bone thickness of teeth numbered 43, 44, and 47. Although the mandibular second molar region was one of the sites where the lowest lingual bone thickness values were observed in our study, the age-related increase observed in tooth number 47 suggests that bone support in this region develops gradually throughout the growth process. This finding is compatible with the bone apposition process accompanying the growth pattern of the mandible and runs parallel to the age-related changes in the anatomical relationship between mandibular third molar germs and the inferior alveolar canal (IAC) reported by Sun et al. [5]. Consequently, the age-dependent increase in bone thickness observed in the mandible indicates that the anatomical relationship between the dental germs and the adjacent neurovascular structures becomes more favorable over time, which leads to a larger safety margin for surgical interventions towards the adolescent period.

While our results indicate specific regions of limited bone support, such as the mandibular second molar lingual area, these results should be interpreted as potential anatomical risk indicators rather than direct evidence of surgical outcome. The establishment of this pediatric reference set may assist clinicians in preoperative risk assessment; however, the actual impact on reducing surgical complications or improving eruption guidance remains to be validated via prospective clinical studies. Our cross-sectional data provide a descriptive framework for understanding the bony envelope surrounding tooth germs, which serves as a baseline for future research on patient-specific treatment planning in pediatric dentistry and orthodontics.

One of the primary limitations of our study is that the axial inclination/angulation of the teeth was not included in the measurements. Plaza-Serrano et al. [23] and Srebrzyńska-Witek et al. [26] reported associations between tooth inclination and surrounding alveolar bone dimensions, including cancellous bone thickness. Although performing this measurement in teeth at the germ stage involves technical challenges, incorporating the factor of axial tooth inclination in future studies could contribute to a more comprehensive explanation of anatomical variations.

Furthermore, as noted by Goshtasbi et al. [24], the fact that 50–58% of the variation in bone thickness is associated with genetic factors may provide a possible explanation for the individual differences observed in our study beyond age and sex. Additionally, the resolution limits of CBCT regarding thin

anatomical structures below 0.5 mm and the associated measurement uncertainties, as pointed out by Schulze et al., should be considered a technical limitation [25].

Finally, due to the retrospective nature of our study, the vertical growth patterns (facial height) and skeletal classes (Class I, II, and III) of the individuals could not be included in the evaluation. Since it is reported in the literature that these factors can influence alveolar bone morphology [7, 17], this situation may be considered a limitation in the interpretation of our findings. Therefore, future studies incorporating variables such as genetic factors, occlusal forces, axial inclinations, and the direction of growth into their models will contribute to a more comprehensive understanding of the dynamics of alveolar bone development during the pediatric period.

5. Conclusions

In conclusion, this study establishes a CBCT-based anatomical reference for cortical bone thickness surrounding developing permanent tooth germs in a pediatric population. Our results show significant differences between tooth types, jaw regions and age, with less influence of sex and bilateral symmetry in this developmental stage. While the age-related results point to dynamic patterns, these should be interpreted as cross-sectional findings across age groups and not as longitudinal trajectories. These findings point to specific regions where thin cortical bone could be a concern in clinical applications. However, the direct clinical utility of these reference values for reducing surgical risks or optimizing orthodontic interventions requires further confirmation through longitudinal and outcome-based investigations.

Abbreviations

CBCT
Cone-beam computed tomography
BBT
Buccal bone thickness
L/PBT
Lingual/palatal bone thickness
FOV
Field of view
DICOM
Digital Imaging and Communications in Medicine
ICC
Intraclass correlation coefficient
CI
Confidence interval
IAC
Inferior alveolar canal

Declarations

Ethics approval and consent to participate

The study was conducted in accordance with the Declaration of Helsinki and approved by the Clinical Research Ethics Committee of Harran University (Approval No. HRU/25.13.31; 14 July 2025). Written informed consent was obtained from the parents or legal guardians of all participants included in the study. All patient data were anonymized before analysis to ensure confidentiality.

Consent for publication

Not applicable.

Competing interests

The authors declare that they have no competing interests.

Funding

This work was supported by Dicle University Scientific Research Projects Coordinatorship.

Author Contribution

H.S.Ş., M.E.D., Ş.A., Y.P.Y. and E.C.T. contributed to the conceptualization of the study. H.S.Ş. and E.C.T. contributed to the methodology. H.S.Ş. performed the validation, investigation, data curation and visualization. M.E.D. and İ.Ş. performed the formal analysis. E.C.T. provided resources, supervised the study, administered the project and acquired funding. H.S.Ş. and Y.P.Y. prepared the original draft. H.S.Ş., M.E.D., Ş.A., Y.P.Y., D.S.T., İ.Ş., M.S.K. and E.C.T. reviewed and edited the manuscript. All authors read and approved the final manuscript.

Acknowledgements

Not applicable.

Data Availability

The datasets generated and/or analyzed during the current study are available from the corresponding author on reasonable request. The data are not publicly available due to ethical and privacy restrictions.

References

1. Menezes CC, Janson G, Massaro CS, Cambiaghi L, Garib DG. Reproducibility of bone plate thickness measurements with cone-beam computed tomography using different image acquisition protocols. Dent Press J Orthod. 2010;15:143–9. 10.1590/S2176-94512010000500017.
2. Zhang S, Liu Y, Li D, Liu J, Wang L, Feng Z. Artificial intelligence- and pediatric CBCT-aided developmental recognition and personalized treatment of periapical diseases. Innov Med. 2025;3:100118. 10.59717/j.xinn-med.2025.100118.
3. Uğurlu M, Kılıç M, Günen Yılmaz S, Sağlam H, Bilgir E. Retrospective evaluation of the gubernacular tract in impacted/unerupted teeth with cone-beam computed tomography. J Innov Approaches Med. 2021;2:29–37. 10.29329/jiam.2021.411.1.
4. Oda M, Miyamoto I, Nishida I, Tanaka T, Kito S, Seta Y, et al. A spatial association between odontomas and the gubernaculum tracts. Oral Surg Oral Med Oral Pathol Oral Radiol. 2016;121:91–5. 10.1016/j.oooo.2015.10.014.
5. Sun R, Cai Y, Yuan Y, Zhao JH. The characteristics of adjacent anatomy of mandibular third molar germs: a CBCT study to assess the risk of extraction. Sci Rep. 2017;7:14154. 10.1038/s41598-017-14144-y.
6. la Zambrano-De LS, Aliaga-Del Castillo A, Rodríguez-Cárdenas YA, Ruiz-Mora GA, Arriola-Guillén LE, Guerrero ME. Bucco alveolar bone thickness of mandibular impacted third molars with different inclinations: a CBCT study. Surg Radiol Anat. 2020;42:1051–6. 10.1007/s00276-020-02447-1.
7. Coşkun İ, Kaya B. Relationship between alveolar bone thickness, tooth root morphology, and sagittal skeletal pattern: a cone beam computed tomography study. J Orofac Orthop. 2019;80:144–58. 10.1007/s00056-019-00175-9.
8. D'Angeli G, Messineo D, Riminucci M, Corsi A, Celli M, Vozza I, et al. The characteristics of adjacent anatomy of mandibular third molar germs: a CBCT pilot study in patients with osteogenesis imperfecta. Healthcare. 2020;8:372. 10.3390/healthcare8040372.
9. Gurler G, Delilbasi C, Delilbasi E. Investigation of impacted supernumerary teeth: a cone beam computed tomograph (CBCT) study. J Istanb Univ Fac Dent. 2017;51:18–24. 10.17096/jiufd.20098.
10. Gürler G, Delilbaşı Ç, Aydın K. Evaluation of unerupted odontomas with cone beam computed tomography (CBCT). J Int Dent Sci. 2016;136–42. 10.21306/jids.2016.1.20.
11. Aldosimani MA, Aljarbou FA, Althumairy RI, Alhezam AA, Aldawsari AI. Analysis of mandibular premolar root position in relation to adjacent cortical plates and mental foramen using cone beam computed tomography in the Saudi population. Saudi Med J. 2019;40:298–301. 10.15537/smj.2019.3.23597.
12. Dinu C, Almășan O, Hedeșiu M, Armencea G, Băciuț G, Bran S, et al. The usefulness of cone beam computed tomography according to age in cleft lip and palate. J Med Life. 2022;15:1136–42. 10.25122/jml-2022-0209.

13. Narmada IB, Putri AR. The effect of maxilla impacted canine positions on root resorption of adjacent teeth using cone-beam computed tomography imaging. Acta Med Philipp. 2024;58:90–7. 10.47895/amp.vi0.4321.
14. Nalbantoğlu AM, Yanık D. Evaluation of facial alveolar bone thickness and fenestration of the maxillary premolars. Arch Oral Biol. 2022;142:105522. 10.1016/j.archoralbio.2022.105522.
15. Adiguzel O, Aktuna Belgin C, Falakaloglu S, Cangul S, Akkus Z. Maxillary cortical bone thickness in a south-eastern Anatolian population: a cone-beam computed tomography study. Med Sci Monit. 2017;23:5812–7. 10.12659/MSM.906229.
16. Shafizadeh M, Tehranchi A, Shirvani A, Motamedian SR. Alveolar bone thickness overlying healthy maxillary and mandibular teeth: a systematic review and meta-analysis. Int Orthod. 2021;19:389–405. 10.1016/j.ortho.2021.07.002.
17. Zhang Y, Wang J, Yin Y, Li P, Xue C, Yang X, et al. Anterior arch form-specific analysis of alveolar bone thickness and tooth inclination: associations and clinical relevance in skeletal class II malocclusion. BMC Oral Health. 2025;25:1783. 10.1186/s12903-025-07121-9.
18. Porto OCL, Silva BSF, Silva JA, Estrela CRA, Alencar AHG, Bueno MR, et al. CBCT assessment of bone thickness in maxillary and mandibular teeth: an anatomic study. J Appl Oral Sci. 2020;28:e20190148. 10.1590/1678-7757-2019-0148.
19. Chi CC, Shen YW, Fuh LJ, Huang HL. Clinical evaluation of tooth angle and peripheral bone thickness considering sex and age for implant placement in the maxillary anterior region. J Prosthet Dent. 2024;132:e7831–7. 10.1016/j.prosdent.2024.04.018.
20. Firincioglulari M, Koral S, Kurt D, Orhan K. Gender-based variation in alveolar bone thickness of maxillary incisor teeth: a CBCT retrospective study. Med Sci Monit. 2024;30:e944588. 10.12659/MSM.944588.
21. Thongudomporn U, Chongsuvivatwong V, Geater AF. The effect of maximum bite force on alveolar bone morphology. Orthod Craniofac Res. 2009;12:1–8. 10.1111/j.1601-6343.2008.01430.x.
22. Iuliano-Burns S, Hopper J, Seeman E. The age of puberty determines sexual dimorphism in bone structure: a male/female co-twin control study. J Clin Endocrinol Metab. 2009;94:1638–43. 10.1210/jc.2008-1522.
23. Plaza-Serrano MA, Robayo-Alvarado SL, Llaguno-Rubio JM, Arriola-Guillén LE. Evaluation of cortical bone thickness in upper central incisors with different types of buccopalatal inclination: a CBCT study. J Contemp Dent Pract. 2025;26:239–43. 10.5005/jp-journals-10024-3833.
24. Goshtasbi N, Hazzard J, Mehrkhodavandi N, Al-Qawasmi R. The heritability of alveolar bone thickness in siblings seeking orthodontic treatment. Am J Orthod Dentofac Orthop. 2020;157:803–8. 10.1016/j.ajodo.2019.06.019.
25. Schulze R, Couso-Queiruga E, Katsaros C. Accuracy of cone-beam computed tomography in imaging the components of the periodontal phenotype. Periodontol 2000. 2024;94:120–35. 10.1111/prd.12556.

26. Srebrzyńska-Witek A, Koszowski R, Różyło-Kalinowska I. Relationship between anterior mandibular bone thickness and the angulation of incisors and canines—a CBCT study. Clin Oral Investig. 2018;22:1567–78. 10.1007/s00784-017-2255-3.

Figures

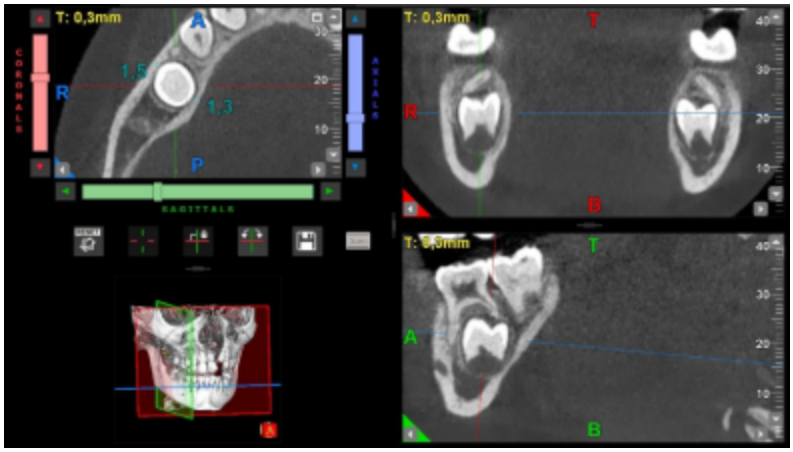


Figure 1

Measurement protocol for the buccal and lingual/palatal bone thicknesses adjacent to developing permanent tooth germs on CBCT slices.